Liquid-Phase and Evanescent-Wave Cavity Ring-Down Spectroscopy in Analytical Chemistry

L. van der Sneppen, F. Ariese, C. Gooijer, and W. Ubachs

Laser Center, Vrije Universiteit, Amsterdam 1081 HV, The Netherlands; email: wimu@nat.vu.nl

Annu. Rev. Anal. Chem. 2009. 2:13–35

First published online as a Review in Advance on November 25, 2008

The *Annual Review of Analytical Chemistry* is online at anchem.annualreviews.org

This article's doi: 10.1146/annurev-anchem-060908-155301

1936-1327/09/0719-0013$20.00

Key Words

absorbance spectroscopy, optical detection, lasers, liquid chromatography, biosensors

Abstract

Due to its simplicity, versatility, and straightforward interpretation into absolute concentrations, molecular absorbance detection is widely used in liquid-phase analytical chemistry. Because this method is inherently less sensitive than zero-background techniques such as fluorescence detection, alternative, more sensitive measurement principles are being explored. This review discusses one of these: cavity ring-down spectroscopy (CRDS). Advantages of this technique include its long measurement pathlength and its insensitivity to light-source-intensity fluctuations. CRDS is already a well-established technique in the gas phase, so we focus on two new modes: liquid-phase CRDS and evanescent-wave (EW)-CRDS. Applications of liquid-phase CRDS in analytical chemistry focus on improving the sensitivity of absorbance detection in liquid chromatography. Currently, EW-CRDS is still in early stages: It is used to study basic interactions between molecules and silica surfaces. However, in the future this method may be used to develop, for instance, biosensors with high specificity.

1. INTRODUCTION

Because of its simplicity and universality, absorbance detection may be the most-used detection method in liquid-phase analytical chemistry. A major limitation of absorbance spectroscopy in general is its limited sensitivity: Using this technique, one measures a small decrease in light intensity ΔI on a large background with intensity I_0. Therefore, the sensitivity of the technique is ultimately determined by the stability of the light source intensity I_0 and the accuracy with which $\Delta I/I_0$ can be measured. From this point of view, a so-called zero-background technique such as fluorescence spectroscopy is much more sensitive: A small fluorescence signal in an otherwise dark environment is far easier to detect, so achievable detection limits are much more favorable compared with absorbance detection. However, a prerequisite for fluorescence spectroscopy is that the analyte must be fluorescent, whereas absorption can be measured for virtually any compound in any solvent. Therefore, the development of direct absorption detection methods with enhanced sensitivity remains an important goal in analytical chemistry. Moreover, absorbance detection, described by the Lambert-Beer law, allows for a straightforward interpretation in terms of absolute concentrations.

When developing a novel method for laser-based absorption spectroscopy as a tool in analytical chemistry, several crucial factors should be kept in mind. First, the system should be user friendly; for example, the optical alignment should be robust. Second, the method should be broadly applicable in different analytical systems. Important questions are whether the detection system can also be used with aggressive solvents or in gradient separation systems in which the liquid-flow composition is continuously changing, and whether the setup is small enough to be implemented in bench-top analytical systems. Third, economic considerations may play a role, and elaborate or expensive laser systems may not be feasible or even desirable.

This review explores the applicability of cavity ring-down spectroscopy (CRDS) to analytical liquid-flow systems. CRDS is an exceptionally sensitive type of absorption spectroscopy that has been extensively operated in gas-phase studies. Recently, liquid-phase CRDS has received much attention, and its potential in analytical chemistry has been demonstrated. It has been shown that compared to conventional absorbance detection, the baseline noise and limits of detection (LODs) in liquid chromatography (LC) can be significantly improved (1–7).

Another mode of CRDS is evanescent-wave (EW)-CRDS, where the exponentially decaying EW associated with a total internal reflection (TIR) is used to probe the sample. This mode of CRDS combines the excellent sensitivity of CRDS with the surface specificity of EW spectroscopic techniques. As with liquid-phase CRDS, the development of EW-CRDS has only recently begun. EW-CRDS has shown its potential in various studies of interactions of analytes with bare silica surfaces (8–18). Modification of the TIR surface (19) may become a useful tool for studying (bio)molecular interactions and in label-free biosensing, analogous to, for example, surface plasmon resonance spectroscopy.

1.1 Enhancing the Sensitivity of Absorbance Detection

To measure the absorption spectrum of a sample, the attenuation of light passing the sample is measured as a function of the wavelength, quantitatively described by the Lambert-Beer law. In liquid-phase studies, the following form is commonly used:

$$-\log \frac{I_l}{I_0} = \varepsilon_\lambda C l. \quad (1)$$

Here ε_λ is the molar extinction coefficient at a given wavelength, I_l is the intensity of light as measured after traveling a distance l through a sample with a concentration C of absorbing molecules,

and I_0 is the intensity of light impinging upon the sample. The outcome (i.e., the absorbance) of a conventional absorption measurement is $\varepsilon_\lambda Cl$ in dimensionless absorbance units (A.U.).

A direct approach for enhancing the sensitivity of absorbance detection is the use of a longer pathlength, as has been elegantly demonstrated using multipass arrangements such as Herriot-type or White-type multipass cells (20, 21). However, this technique has some constraints in analytical systems. For instance, to avoid additional bandbroadening in LC, as well as in other liquid-flow analytical techniques, the detection cell volume should not be larger than the injection volume (22). Therefore, such multipass cells are usually too large for analytical purposes. To maintain small detection volumes, one can use narrow liquid-core waveguides (23, 24), in which a hollow-core optical fiber is filled with the sample or is coupled to an LC separation. This way, sample cell lengths can be significantly increased, and a cell volume of several or several tens of microliters can be maintained.

Alternatively, different measurement schemes for laser-based nonfluorescence absorbance detection can be used in analytical flow systems (25). Thermooptical measurement schemes, such as thermal lensing spectroscopy (26, 27), photoacoustic spectroscopy (28, 29), and degenerate four-wave mixing (30, 31) all require that the solvent be heated upon light absorption, followed by energy dissipation by the solute. A major drawback of these thermooptical techniques is they cannot accommodate gradient elutions. In LC in particular, such gradients are widely applied, so the applicability of the abovementioned measurement schemes is severely limited.

As we outline in the next section, CRDS is an elegant and sensitive mode of absorption spectroscopy, circumventing many of the abovementioned disadvantages. The technique was originally developed for a goal quite different from absorbance spectroscopy. Setups for mirror reflectivity measurements (32, 33) serendipitously turned into a sensitive absorption detection method. The recognition of the potential for measuring molecular properties through probing ring-down events from an optical resonator may be considered as marking the advent of CRDS (34). Initially, CRDS was applied only in gas-phase studies, where its excellent sensitivity levels are rivaled only by photoacoustic spectroscopy. Reviews on gas-phase CRDS, including variants such as phase-shift CRDS, polarization-dependent CRDS, noise-immune cavity-enhanced optical heterodyne molecular spectroscopy, and broadband CRDS have been published (35–42).

Gas-phase applications of CRDS have matured beyond the level of laboratory spectroscopy. Such applications include noninvasive breath analyzers, which can analyze exhaled breath directly without the need for sampling and preconcentration or pretreatment procedures. An example is online measurement of the $^{12}C/^{13}C$ ratio in exhaled CO_2 after a patient had been given ^{13}C-enriched urea (a marker for bacteria causing stomach ulcers) (43). A breath analyzer for the detection of exhaled ethane (a marker for oxidative damage to tissue, which plays a role in diseases such as cancer and atherosclerosis) has also been developed, demonstrating that 500-ppt detection levels are feasible (44, 45). The application of different CRDS schemes to condensed media has recently attracted much interest (46). Later in this review, we describe some additional recent developments of CRDS detection in the liquid phase and on surface layers.

1.2. The Cavity Ring-Down Spectroscopy Technique

The principle of CRDS is illustrated in **Figure 1**. The core of a CRDS setup is a cavity composed of high-reflectivity dielectric mirrors; reflectivities can be on the order of 99.9% or even 99.99%. The stacked reflective layers have a thickness of a quarter of the design wavelength, so reflections from consecutive layers are in phase. Therefore, the mirrors work best at the design wavelength and are relatively narrowbanded. Typically, a range of approximately 10% around a chosen center wavelength can be used for meaningful CRDS measurements.

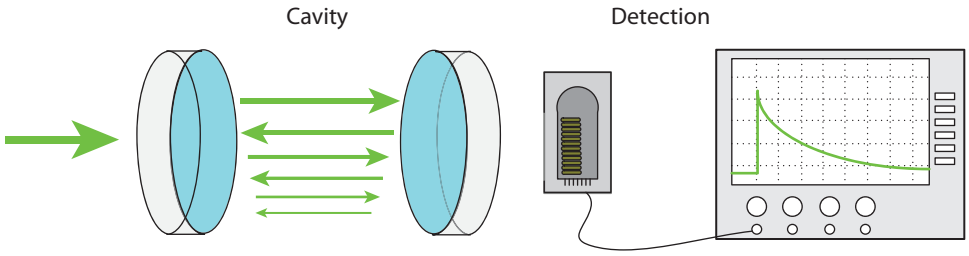

Figure 1

The principle of cavity ring-down spectroscopy (CRDS). After abrupt termination of the excitation, the light stored in the cavity decays exponentially as it bounces back and forth between the mirrors, losing some intensity at each reflection. The decay rate of the light can be measured behind the cavity.

The CRDS technique (ignoring interference) can be summarized as follows: If the entrance mirror of a cavity has a reflectivity of R, a fraction (1 − R) of light incident on the mirror is transmitted and enters the cavity, provided that scatter losses are negligible. After abrupt termination of the excitation, the stored light bounces back and forth between the two mirrors, losing 1 − R at each reflection (see **Figure 1**). Light leaking out of the cavity after each bounce results in an exponential decay of light intensity exiting at the rear of the optical cavity; this decay can be detected, digitized, and fitted to an exponent. The ring-down time (1/e) is a measure of the reflection and scatter losses of the cavity. When an absorber is present in the cavity, additional light is lost due to absorption, and the ring-down time becomes shorter.

The signal measured in CRDS (a monoexponential decay) is similar to the actual phenomenon of absorption, which can also be described by a monoexponential decay using the Lambert-Beer law. Indeed, the absorbance can be directly derived from the measured ring-down time via

$$\varepsilon_\lambda C l = \frac{n_{avg} L}{2.303 c}\left[\frac{1}{\tau} - \frac{1}{\tau_0}\right], \qquad (2)$$

where τ and τ_0 are the ring-down times in the presence or absence of analyte, respectively. Subtraction of the baseline loss τ_0^{-1} is necessary to account for the reflection and scatter losses. n_{avg} is the average refractive index if more than one medium is present in the cavity, L is the cavity length, and c is the speed of light.

Technically, it is not the decrease in light intensity due to absorption that is measured, but rather the decay rate of light leaking away behind a cavity. Therefore, CRDS is insensitive to intensity fluctuations of the light source. Furthermore, the multipass nature of CRDS ensures a long effective pathlength: Light that exits from the cavity after a ring-down time τ has traversed the sample hundreds or thousands of times, resulting in pathlengths measuring up to meters or even kilometers. In contrast to the Herriot-type or White-type multipass cells discussed above, the position of the traversing laser beam does not change during measurements and probes the same sample volume on each round trip; thus, the system may be miniaturized. The absorbance can be directly deduced from the measured τ, provided that the cavity length is known. If the cavity is entirely filled with the absorbing medium (hence $L = l$), the εC product can be measured without having knowledge of the cavity length.

The main strength of CRDS is its excellent sensitivity; CRDS is commonly utilized in trace analyses or for the measurement of molecular transitions with a low transition probability. However, concentration ranges of only two to three orders of magnitude can be accommodated due to limitations in the dynamic range of analog/digital conversion under ultrafast

conditions. In effect, the amount of data that can be used for extracting a fitted τ is restricted to fewer than five decay times, irrespective of the specific value of τ. This is not a serious drawback: for samples with high absorbances, more conventional techniques can be considered as alternatives.

1.3. Combining Absorbance Detection with Surface Sensitivity and Specificity

When a TIR event on an interface between two media takes place, a small portion of light (the EW) penetrates the less dense medium. The EW decays exponentially, and the penetration depth—which is dependent on the angle of incidence, the refractive indices of the two media, and the wavelength used—is typically on the order of one wavelength. Unsurprisingly, the EW can be exploited for spectroscopic studies, with the advantage that only molecules present at or near the surface of the dense medium are probed. Therefore, EW spectroscopic techniques are surface specific and are especially suitable for the measurement of interactions occurring at surfaces.

Because of the short effective pathlength through the sample, EW absorbance signals are relatively weak. The inherently low sensitivity of EW absorbance spectroscopy can be enhanced by using multiple TIR events for one measurement. This can be accomplished with attenuated total reflectance (ATR) prisms (**Figure 2*a***) (47), which usually accommodate several tens of TIR events. However, ATR prisms commonly measure several centimeters long, so large sample volumes are required. Another option is the use of fibers or waveguides, of which part of the cladding is stripped off to expose the core and thus the EW of the light propagating in the core (**Figure 2*b***) (48–50). Because waveguides can be much smaller than ATR prisms, this approach is more suitable for miniaturization.

A third option is the use of EW-CRDS, a schematic of which is depicted in **Figure 2*c***. In this approach, one of the reflections inside the CRDS cavity is a TIR event, and only the light associated with this TIR event is utilized for probing the sample. Advantages of EW-CRDS over the conventional ATR and waveguide techniques include its multipass nature and its insensitivity to light-source-intensity fluctuations. Unlike ATR and waveguide spectroscopies, EW-CRDS lends itself perfectly to miniaturization because the same spot at the interface (and therefore an extremely small volume) is repeatedly probed. Some schemes of EW-CRDS also permit polarization-dependent studies, which in turn allows for molecular orientation studies.

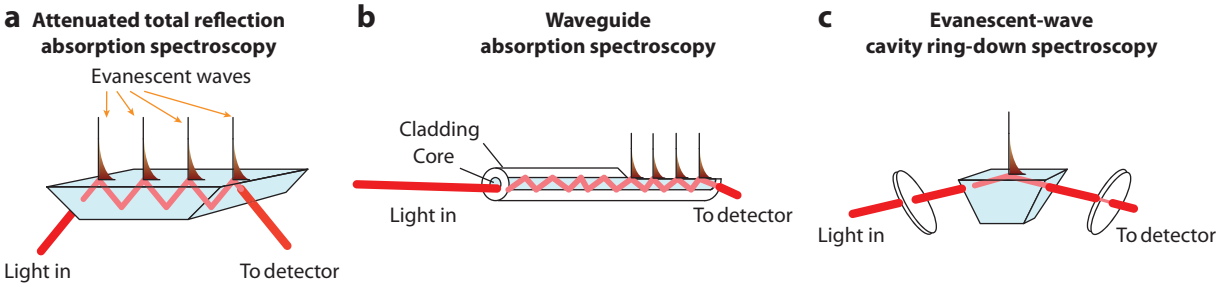

Figure 2

Different modes of evanescent-wave absorption spectroscopy. (*a*) Attenuated total reflectance absorption spectroscopy. (*b*) Waveguide absorption spectroscopy. (*c*) Evanescent-wave cavity ring-down spectroscopy. The samples, which have a lower refractive index than the media that carry the propagating light (*light blue*), are placed on top of the interfaces, where total internal reflection occurs.

2. CAVITY RING-DOWN SPECTROSCOPY: PRINCIPLES AND TECHNIQUES

To use an optical resonator in a ring-down experiment, the stability criterion of a cavity must be fulfilled (51):

$$0 < \left(1 - \frac{L}{R_c}\right)^2 < 1. \tag{3}$$

Here R_c is the radius of curvature of the mirrors, and L is the cavity length. The mode structure of a cavity is given by

$$\nu = \frac{c}{2L}\left[q + (m + n + 1)\left(\frac{1}{2} + \frac{2}{\pi}\arctan\frac{L - R_c}{L + R_c}\right)\right], \tag{4}$$

where q is the longitudinal mode number and m and n refer to the transversal modes (52). If the transverse modes are suppressed, the equation takes the form of the equally spaced ($\Delta\nu = \frac{c}{2L}$ spaced) transmission fringes of an etalon; this condition can be most easily met under confocal conditions ($L = R_c$). If transversal modes are excited, and if the resonator length is sufficiently far away from the confocal condition, the filling-in of transverse modes may become so dense that the resonator becomes a white-light attenuator/transmitter (53). This condition is particularly useful for cavity ring-down experiments, as the transmission of the resonator (and therefore the ring-down properties) becomes wavelength independent. This behavior of the resonator was experimentally demonstrated using a typical ring-down configuration for $L = 1.15R_c$ (54). In this configuration, all the modes contained in the output of a broadband pulsed laser equally contribute to the ring-down phenomena: This is multimode CRDS.

2.1. Multimode Excitation

The most straightforward implementation of CRDS is multimode excitation of the cavity. In multimode excitation, the spectral bandwidth of the laser pulse is much larger than the free spectral range (FSR) of the cavity. The coherence length of the laser pulse must be much shorter than the length of the cavity; this condition is usually satisfied through the use of a non-single-mode optical parametric oscillator (OPO) or a pulsed dye laser. The best results are achieved if the transverse modes of the cavity, in addition to the longitudinal modes, are also excited: Modulation on the ring-down then washes out. Due to the white transmission spectrum of the cavity, continuous absorption spectra can be recorded. Under such conditions, typical shot-to-shot fluctuations of 1% or better on the obtained ring-down times can be obtained. In liquid-phase studies, where absorbance features are usually several tens of nanometers wide, spectral bandwidth does not pose a problem.

2.2. Single-Mode Excitation

If only a single transversal mode of the cavity is excited, the output-mode spectrum of the laser and the transmission-mode spectrum of the cavity should coincide. To suppress higher-order transversal modes, the use of a confocal cavity, as well as mode-matching, is advantageous. Because single-mode excitation yields a purely monoexponential decay transient, decay times can be fitted extremely precisely: Standard deviations of the ring-down time are on the order of 10^{-4}, compared to 1% for multimode CRDS. As a result, single-mode CRDS is more sensitive than the multimode variant.

Single-mode CRDS can be performed using a narrowband pulsed laser (55), but it is usually carried out with continuous-wave (CW) lasers. There are a variety of approaches for single-mode

excitation. One option is to lock one of the modes of the cavity to the narrow bandwidth output of a laser using a feedback loop (55). A simpler approach is to sweep the cavity length over one FSR. The laser excitation is actively switched off when the cavity begins to transmit light (using, for example, an acoustooptic modulator) to measure a decay transient (56–58).

2.3. Cavity-Enhanced Absorption Spectroscopy

In cavity-enhanced absorption spectroscopy (CEAS), a CW light source is used to measure the conventional $\Delta I/I_0$ absorbance signal (59–61). A conventional absorption spectrometer can easily be adapted for a CEAS setup with the addition of two mirrors forming a cavity around the sample (62). The use of a laser is not mandatory: Incoherent broadband (IBB) sources such as light-emitting diodes (LEDs) can also be used (63). Because the decrease in integrated light intensity (rather than its time-resolved decay) is measured, a cheaper detection and read-out system can be employed; a simple plug-and-play spectrometer is sufficient (64). To ensure that enough light reaches such a detector, especially when using IBB excitation, the cavity finesse should be low. Thus, extremely high-quality mirror reflectivities are not essential. Using broadband excitation in conjunction with a spectrometer allows for rapid measurement of a complete spectrum without scanning. Although the effective pathlength is shorter, the multipass nature of the technique is maintained. IBB-CEAS is therefore appropriate for miniaturization as well, as the same sample volume is repeatedly probed. However, such a low-cost approach has some disadvantages. First, IBB-CEAS is not immune to light-source-intensity fluctuations, making it inherently less sensitive than the abovementioned multimode and single-mode CRDS techniques. Second, the measurements must be calibrated because the effective pathlength decreases at higher analyte concentrations. This decrease causes deviations from linearity, but it also results in a larger dynamic range (65).

3. CAVITY RING-DOWN SPECTROSCOPY FOR LIQUIDS AND THIN FILMS

Inserting a condensed medium into a cavity is not an easy task. For instance, inserting a cuvette inside the cavity requires the presence of four additional surfaces, which lead to strong reflection and scatter losses. Several options to decrease these losses have been proposed. Thin films can be deposited on substrates that are placed under 90° in the cavity, as has been demonstrated for a C_{60}-coated substrate (66). On each pass, 4% of the light is reflected. However, if the substrate is well aligned, the reflected light can be maintained in the cavity (i.e., the various embedded cavities are optically stable). In another application, single-mode CRDS was used to measure an infrared spectrum of the C–H stretching vibration of alkylsiloxane monolayer films grafted on a silicon substrate placed under normal incidence. The measured absorbance was position dependent; it was maximized at the antinodes of the standing wave in the cavity, whereas it was absent at the nodes (67). It is also possible to deposit thin films directly onto the cavity mirrors (68), although mirror degradation is possible; thus, irreversible deposition techniques such as ion beam sputtering cannot be utilized.

For liquids, one can avoid using additional surfaces by (*a*) filling the entire cavity with liquid [in this case, the mirrors are in direct contact with the liquid (1)], (*b*) placing a cuvette under Brewster's angle in the cavity, thus diminishing reflections (69), or (*c*) aligning a cuvette under 90° in such a way that reflection losses are maintained in the cavity (70). These three approaches have been applied to liquid-phase CRDS studies (see Section 3.1) as well as to LC-CRDS detection (see Section 3.2).

An appealing alternative to conventional mirror-based cavities is the use of fibers. In this approach, fiber-Bragg gratings act as mirrors or fibers are looped upon themselves. Fiber or fiber-loop CRDS can be employed for liquid-phase measurements simply by leaving a gap allowing for a liquid flow (Section 3.3). EW-CRDS (discussed in detail in Section 4) is also feasible; for example, one can remove the fiber cladding and expose the fiber core to the sample (see Section 4.3).

3.1. Liquid-Phase Cavity Ring-Down Spectroscopy Measurements

In the first demonstration of liquid-phase CRDS (69), a spectrum of the fifth overtone of the C–H stretch vibration of benzene was recorded, demonstrating this method's excellent sensitivity compared to that of conventional absorbance spectroscopy. The authors inserted one or two standard cuvettes into the cavity under Brewster's angle. Because the interfaces involved (from air to glass and from glass to liquid) have different Brewster's angles, reflection losses could not be fully prevented, but they could be minimized by placing the cuvette under some intermediate angle in the cavity. As expected, the angle of the cuvette required optimization after every change in the refractive index of the liquid (69).

As mentioned above, intracavity surfaces can be circumvented by filling the entire cavity with liquid (1, 71, 72). Importantly, early studies using a liquid-filled cavity revealed that the mirror reflectivities did not exhibit degradation when in contact with the liquid and that neither stirring nor applying a continuous flow posed a disadvantage. The signal-to-noise ratio was comparable to the Brewster's-angle cuvette approach mentioned above (1, 69). In subsequent studies, the repetition rate of the system was increased from 10 Hz (1) to 10 kHz using a CW-CRDS approach (71, 72). Whereas one may expect a signal-to-noise ratio improvement of a factor of 30 (from the 1000-fold increase of the repetition rate), the investigators obtained only a threefold increase. This modest increase may be due to signal averaging prior to fitting: Because the speed of data transfer and handling is commonly limited to several kilohertz, traces must be averaged on the read-out system prior to data transfer and handling (1, 71, 72), which results in loss of information.

Liquid-filled cavities have been utilized for studying the reduction kinetics of methylene blue by ascorbic acid (71). A concentration of only 3 nM of methylene blue was sufficient for obtaining a reliable reduction curve (71, 72). Although the reduction of methylene blue is a relatively slow process (measurements were performed on a timescale of minutes), CRDS detection can also be used for studying the reaction kinetics of short-lived species such as the NO_3 radical (73). In this study, nitrate radicals were photoinduced by photolysis inside a cuvette placed under Brewster's angle in a linear cavity. At the same time, the reaction of the nitrate radicals and monoterpenes was followed online by monitoring the absorbance decrease. For terpene solutions with various concentrations, the monoexponential ring-down curve in the absence of the photolysis pulse was compared to the biexponential ring-down curve measured in the presence of the photolysis pulse. Thus, the first-order reaction rate constant was determined (73).

As an alternative to introducing liquids into a cavity without the need for intracavity surfaces or direct contact with the mirrors, one can utilize a flowing liquid sheet-jet in a linear cavity (74). A favorable baseline noise level of 0.5×10^{-7} A.U. was obtained, resulting in a 71-nM LOD of a good absorber in a flow of 3.4 ml s^{-1}. Unfortunately, the high flow rates and viscosity necessary for creating a stable liquid flow, as well as the unfavorable optical pathlength through the jet, restrict the use of a flowing liquid-sheet jet in analytical systems.

With some minor adjustments, a commercial bench-top double-beam absorption spectrometer utilizing a xenon arc lamp was rebuilt as an IBB-CEAS setup (65). Two mirrors, forming a stable linear cavity, were placed in the probe beam. A third mirror with a transmission equal to that of the cavity was placed in the reference beam, resulting in a sensitivity for the IBB-CEAS measurements

that was 10-fold greater than that of the conventional single-pass measurements (65). Its baseline noise level (approximately 10^{-5} A.U.) was comparable to that of a similar system utilizing LEDs for excitation and a small-scale spectrometer (64). The use of mirrors with relatively low reflectivities (approximately 99%) was found to be advantageous for the sensitivity of the measurement, as more light reaches the detector. Such low-reflectivity mirrors are applicable over a broader wavelength range; thus, IBB-CEAS is suitable for recording broad absorption features (64, 75). Sensitivities obtained with CEAS using a CW laser can even be slightly better than those obtained with pulsed multimode CRDS (76, 2): Using a microliter-sized liquid-filled cavity, a baseline noise level of 2×10^{-6} A.U. was obtained (76), and subnanomolar concentrations of bacteriochlorophyll *a* were detected. However, such a setup does not benefit from the main advantages of CEAS, namely its simplicity and its applicability to a broad wavelength range.

3.2. Cavity Ring-Down Spectroscopy for Liquid Chromatography Detection

Many LC analyses aim to obtain a highly resolved chromatogram and to determine the retention times of the various analytes at low concentration levels. Rather than scanning the wavelength, one monitors the absorbance at a particular wavelength in a continuous flow (see **Figure 3**). Because sample sizes in analytical chemistry are often on the order of several microliters to nanoliters, and to prevent bandbroadening, detection volumes in LC should be microliter sized or smaller. Relatively large liquid-filled cavities (1, 71–73) or liquid-sheet jets (74) thus cannot be used. Furthermore, LC detection cells should permit a continuous, preferably laminar flow. The three different approaches for introducing a liquid into a cavity (discussed above) have also been adapted for use in LC with CRDS detection (see **Figure 4**). Zare and colleagues (2, 3) designed a flow-cell with the correct Brewster's angle for all four interfaces. The feasibility of using a liquid-only cavity (5, 6) as well as a commercial flow-cuvette under 90° (7) has also been demonstrated.

Utilizing the Brewster's-angle flow-cell (see **Figure 4*a***), both pulsed multimode CRDS at 10 Hz (2) and single-mode CW-CRDS at approximately 30 Hz (3) have been performed. As expected, the single-mode variant is the most sensitive: The peak-to-peak baseline noise in LC separations was only 2×10^{-7} A.U., whereas that for multimode CRDS was 3.2×10^{-6} A.U. **Figure 5** depicts the chromatogram obtained for the separation of a test mixture of anthraquinones with CW-CRDS detection. The baseline noise is shown to be much better than that obtained with the commercial detector; however, because of the unfavorable pathlength of the Brewster's-angle flow-cell (0.3 mm, compared to 10 mm for the commercial absorbance detector), the obtained concentration detection limits do not show significant improvement (3). The Brewster's-angle flow-cell depicted was designed for liquids with one specific refractive index. Hence, the use of a gradient elution (where the refractive index is continuously changing) would adversely affect the baseline noise and the sensitivity of the system. However, refractive indices of most common LC solvents are similar, and this effect would probably be small.

It has been shown that for liquids commonly used as solvents in LC, direct contact with high-reflectivity mirrors does not adversely affect their reflectivities, and there appear to be no long-term exposure effects (1). These observations formed the basis for the development of a liquid-only cavity that can be used as a detector in LC studies (see **Figure 4*b***) (4). The baseline noise of the pulsed multimode CRDS setup is comparable to that obtained by the Zare group (2), but due to the larger optical pathlength through the sample, more favorable LODs (on the order of 15- to 20-nM injected concentrations) are obtained (**Figure 3**) (2, 3, 5). The cavity length measures only 2 mm; the ring-down times are therefore short, necessitating a short instrumental response function (e.g., the use of a picosecond laser and a fast detector). Fortunately, with the speed of currently available detection and read-out systems, this is not a serious constraint. The advantage of a system in which

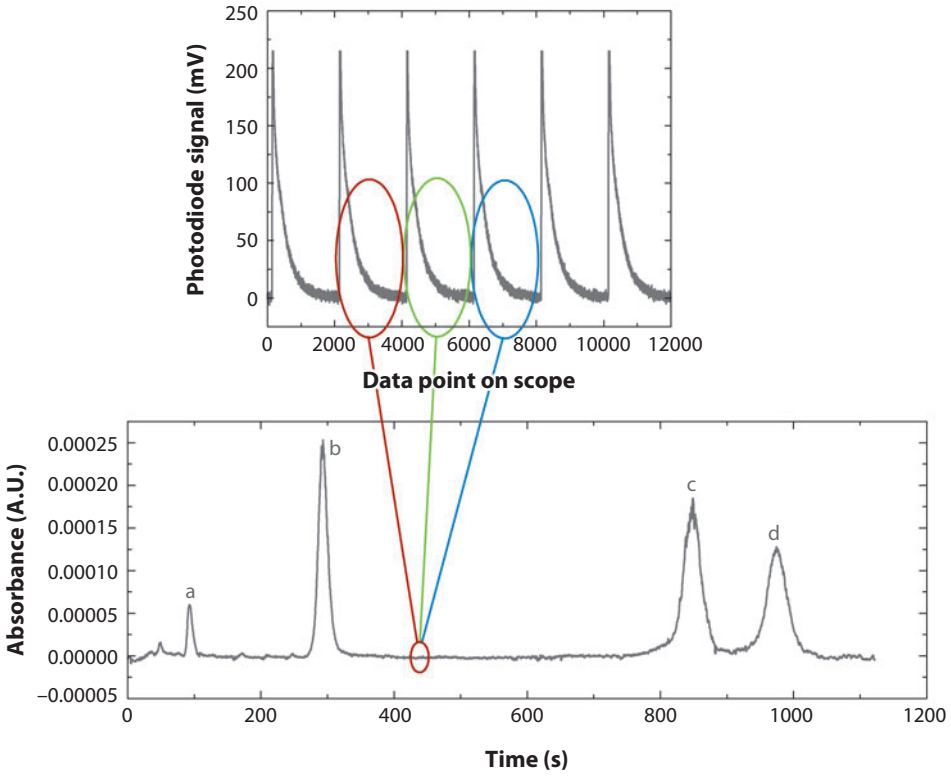

Figure 3

The principle of cavity ring-down detection in liquid chromatography. Ring-down traces are recorded and fitted online during elution of the eluent-containing separated components, resulting in a chromatogram. The sample is a mixture of three azo dyes: direct red 10 (*b*), benzopurpurin (*c*), and chlorazol azurin (*d*). The first peak (*a*) on the chromatogram represents an impurity present in direct red 10 dye. Each dye has a concentration of 300 ppb; the measurement wavelength is 532 nm. The complete experiment is described in Reference 5. Abbreviation: A.U., absorbance units.

the round-trip time is fully utilized for probing the sample is that repetition rates, in principle, can be increased up to the megahertz range, thus increasing the signal-to-noise ratio and the sensitivity.

Because most analytes absorb in the ultraviolet range, it is essential to test CRDS detection not only in the visible range, but at shorter wavelengths as well. The main challenge faced when using CRDS at shorter wavelengths is the poor quality of the available mirrors. Lower mirror reflectivities are accompanied by even shorter ring-down times, so the liquid-only cavity approach is not suitable. Ring-down times can be elongated by increasing the round-trip time, for instance by placing a cuvette inside a relatively long linear cavity (**Figure 4*c***). The reflectivity of the mirrors at 355 nm was still sufficient for using the liquid-only cavity, and as expected, the system's performance was a factor of 10 lower than that in the visible range (5, 6). The baseline noise obtained for LC-CRDS detection using the flow-cuvette at 355 nm was comparable to that of the liquid-only cavity at the same wavelength, but the LODs were slightly better due to the longer optical pathlength through the sample (10 mm instead of 2 mm) (6, 7). Although the principle of LC-CRDS could have been experimentally extended to wavelengths of 273 nm, the available mirrors at these deep-ultraviolet wavelengths, compared to those of conventional LC absorbance

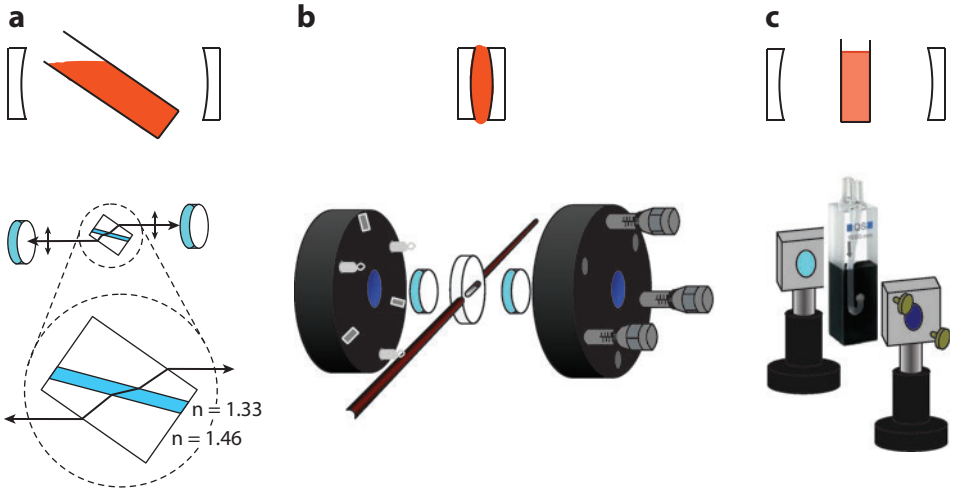

Figure 4

Three geometries for implementing cavity ring-down spectroscopy as a detector in liquid chromatography. (*a*) The Brewster's-angle flow-cell in a linear cavity. (*b*) A miniature liquid-only cavity. When in operation, the left and right segments holding the mirrors are clamped leak-tight around the silicon rubber flow-cell. (*c*) A commercial flow-cuvette in a linear cavity. Brewster's-angle flow-cell adapted from Reference 2.

detectors, were too low in reflectivity ($R \geq 99.91\%$) to improve sensitivity (7). Future advances in mirror-coating technology may improve the sensitivity of CRDS in the deep ultraviolet.

3.3. Optical Fiber Cavities

Optical fibers that are looped upon themselves can act as an optical cavity. Light is coupled into and out of the fiber loop using commercially available input and output couplers. A liquid flow-cell

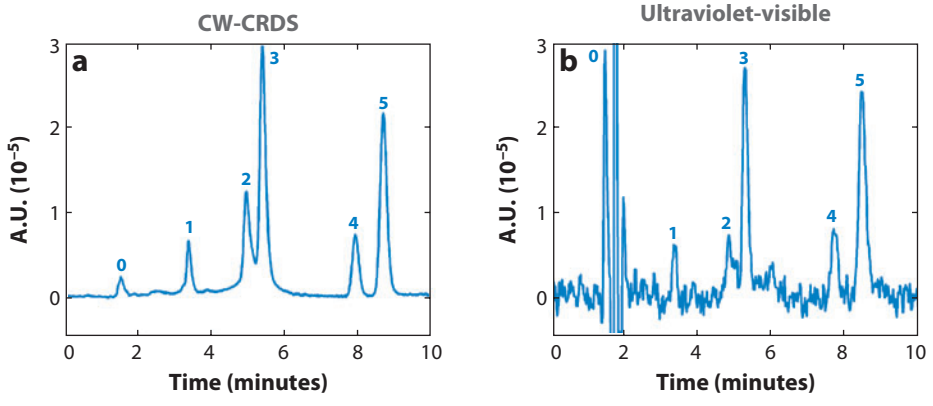

Figure 5

Continuous-wave–cavity ring-down spectroscopy (CW-CRDS) detection of the separation of a test mixture of anthraquinones (0, solvent peak; 1, alizarin; 2, purpurin; 3, quinalizarin; 4, emodin; 5, quinizarin) compared to a state-of-the-art commercial ultraviolet-visible absorbance detector with a pathlength of 10 mm (33 times longer than the Brewster's-angle flow-cell). Reproduced with permission from Reference 3. To account for the pathlength difference, the detection with CW-CRDS (*a*) is compared to the detection of sample that was 33 times diluted in the ultraviolet-visible detector (*b*). Copyright 2005, American Chemical Society.

can easily be inserted into this cavity via a commercially available splice connector; the index-matching fluid of the splice connector is replaced by the sample to be measured (77). Because the capillaries commonly used in capillary electrophoresis (CE) have much smaller volumes than do LC columns, their detection cell volumes are subject to even more severe constraints. Because of the small dimensions of fiber cores, the volumes of these detection cells can be made as small as several picoliters, thereby allowing for CE detection (78).

The principle of liquid-phase fiber-loop systems can be combined with various modes of CRDS, such as phase-shift CRDS (79). In this mode, the phase-shift of a sinusoidally intensity-modulated CW laser (rather than a ring-down transient) is measured after stopping the excitation of the optical resonator. This technique is somewhat similar to CEAS in that the total transmitted light is used for the measurement. Because the absorption measurement is based on the phase-shift of this integrated light, phase-shift CRDS is less sensitive to light-source-intensity fluctuations than is CEAS. LODs using the phase-shift fiber-loop CRDS are on the order of several micromolars for a strong absorber—a 45-fold improvement over the pulsed fiber-loop CRDS setup, where a flow-cell with a 10-times-shorter optical pathlength was used (77, 79).

Phase-shift fiber-loop CRDS has been applied as a detector in CE (80). Injections of different dye concentrations in a continuous flow demonstrate that the response of the phase angle is linearly dependent on concentration, with LODs on the order of several micromolars. To test the performance of fiber-loop CRDS detection in an actual CE separation, different concentrations of the protein human serum albumin (HSA) were noncovalently bound to a dye at a fixed concentration. The resulting mixtures containing unbound dye and dye-labeled HSA were separated, revealing a submicromolar LOD for the labeled HSA (80). Another option is excitation with a tunable gain-switched diode laser delivering picosecond pulses followed by detection of a ring-down transient, but this technique resulted in less favorable detection limits (81).

4. EVANESCENT-WAVE CAVITY RING-DOWN SPECTROSCOPY

CRDS measurements can be straightforwardly combined with surface specificity if one of the reflections in the cavity is a TIR event and if only the EW associated with this TIR event is used for probing the sample. Because introducing a TIR surface into a cavity is quite similar to introducing a liquid, one can utilize similar approaches. The most elegant solution for minimizing reflection losses at intracavity surfaces is discussed in detail in Section 4.1: Reflection losses are circumvented altogether by using a so-called folded resonator, a prism with the cavity mirrors deposited on the entrance and exit faces. The cavity-stability criterion can be fulfilled by spherically polishing one of the prism surfaces, such as the TIR surface.

Alternatively, one can use a prism with entrance and exit faces at 90°, thus maintaining reflection losses in the cavity. A third option is to utilize a conventional 45° Dove© prism with a high-quality antireflective coating. Finally, minimization of reflection losses can be achieved by using a Brewster's angle for the entrance and exit faces. The different approaches involving intracavity prisms are discussed in Section 4.2.

A major advantage of using EW-CRDS with the ring or folded resonators and the prism with 90° entrance and exit faces is the ability to determine the average orientation angle of molecules that are adsorbed to the TIR interface by measuring the difference in absorption between p- and s-polarized light. Because the intracavity 45° antireflective Dove prism and the Brewster's-angle prism are optimized for one polarization only, these geometries cannot be used for molecular orientation studies.

4.1. Evanescent-Wave Cavity Ring-Down Spectroscopy Using Folded Resonators

Following the development of a monolithic resonator (82), Pipino et al. (8) designed a ring resonator suitable for EW-CRDS measurements (**Figure 6*a***). The polarization-dependent absorption of I_2 (deposited from saturated iodine vapor on one of the silica TIR faces) was measured at 580 nm. An impressive minimum detectable surface coverage of 0.006% of an I_2 monolayer, as well as the average orientation angle of the iodine molecules, was determined (9). The optical losses of the ring resonator caused by the absorption of the resonator material (Heraeus Suprasil© fused silica) decrease significantly upon shifting to the near-infrared, where fused silica is the most transparent. Whereas the round-trip intrinsic loss is between 500 and 100 ppm in the wavelength range of 450 to 580 nm, it is less than 40 ppm in the near-infrared (9, 83). To demonstrate the broad applicability of the ring resonator in the latter wavelength region, the first and second OH-stretching overtones of HNO_3 adsorbed on silica were measured in the wavelength range of 1212 to 1653 nm. The excitation source was a broadly tunable Nd:YAG-pumped OPO, and the complete spectrum was measured in a single run without changing the measurement setup (83).

An alternative to the monolithic ring resonator is depicted in **Figure 6*b***. Here, the entrance and exit faces of a 45° prism are covered with high-reflectivity coatings. The design and optical alignment of this system are relatively straightforward. However, it has a disadvantage: It lacks wavelength tunability, as the high-reflectivity coatings are narrowbanded. In a proof-of-principle experiment, the iodine measurement on the ring resonator (described above) (9) was repeated using a folded cavity with mirror coatings centered at 520 nm (10). The optical round-trip losses of the system, as well as the minimum detectable iodine surface coverage, were comparable to that of the ring resonator in the wavelength range of 490 to 540 nm. In a subsequent study using a folded cavity with mirror coatings centered at 1652 nm, the first C–H stretching overtones

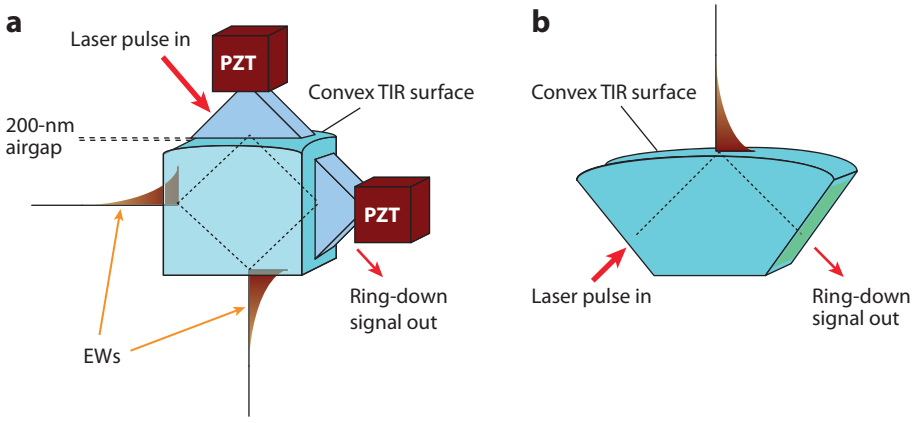

Figure 6

(*a*) A total internal reflection (TIR) ring resonator (adapted from Reference 8). One side of the fused-silica cube is spherically polished in order to maintain a stable cavity. In one round trip, the laser pulse strikes the three flat surfaces and the spherical surface so that the two sides without incoupling and outcoupling prisms can be used for measurements. (*b*) Schematics of a folded resonator for evanescent-wave cavity ring-down spectroscopy (EW-CRDS) measurements (adapted from Reference 84). The mirrors are coated directly on the entrance and exit faces of a 45° prism, thereby avoiding optical losses. The TIR surface of the prism is equipped with a convex superpolish in order to maintain a stable cavity.

of trichloroethylene and *cis*- and *trans*-dichloroethylene were probed, and the absolute surface coverages as well as the average molecular orientations were determined (85).

An advantage of the folded cavity is the straightforward alignment of the system, which allows good measurements even if the sample is isolated from the excitation source and the detection system (e.g., in an ultrahigh vacuum or in a low-humidity chamber). Using mirror coatings centered at 1205 nm, the $2\nu OH + \delta OH$ vibration-combination bands of surface hydroxyls as well as of surface-bound water were probed (84). The observed polarized $2\nu OH + \delta OH$ doublet, assigned to the geminal surface hydroxyls [Si–$(OH)_2$ groups], indicated the presence of an extended H-bonded network of the germinal hydroxyls. Furthermore, in addition to these crystalline β-crystoballite (1,0,0)–like domains, a weak peak assigned to a tilted surface hydroxyl species indicated the presence of fewer crystalline (1,1,1)–like domains. Upon exposing the relatively dry, quasi-crystalline surface to a high-humidity surrounding, an ordered monolayer of water formed on the surface (84). This study convincingly demonstrated that EW-CRDS has sufficient sensitivity for detecting monolayers, but the results regarding the observed extended network of geminal and isolated hydroxyl groups are less definite. In this case, the fully hydroxylated surface was crystalline. However, a less-crystalline partially or fully hydroxylated surface (e.g., an amorphous silica or quartz surface) can be expected to behave quite differently (86). In both cases the surface will be fully hydroxylated; in fact, the exact structure of the silica surface (partially or fully β-crystoballite or quartz) will depend on the history of the sample and on the hydroxylation procedure applied.

The same folded resonator with mirror coatings centered at 1205 nm has been utilized as an in situ probe for measuring dangling bond defects during growth of a hydrogenated amorphous silicon (*a*-Si:H) thin film on the TIR surface of the resonator (87). Such films play an important role in the development of low-cost flexible solar cells, but mechanistic insight into the exact growth mechanism of the deposited films is limited. The surface radical sites (the so-called dangling bonds) are generally believed to be growth sites for the thin film; the absorption of these surface dangling bonds, as well as of bulk dangling bonds, was probed with the folded resonator. It has been shown that the creation rate of the surface dangling bond during thin-film growth was 60 times too small to account for the actual growth rate (87).

The folded resonators designed by Pipino (9, 10, 85, 87) for gas-phase studies utilize a reflection angle at 45°; this angle does not provide for TIR when a liquid is placed on the TIR face of the prism, due to the increased refractive index of the liquid frustrating the TIR phenomenon. A straightforward adjustment of the resonator design, for example using a 70° folded cavity, would allow for liquid-phase EW-CRDS studies. As of now, however, no such studies have been performed. As we discuss in the next section, liquid-phase EW-CRDS measurements are currently performed using intracavity elements with relatively high losses, implying that the baseline noise is usually not better than 10^{-4} or 10^{-5} A.U.

4.2. Intracavity Elements for Evanescent-Wave Cavity Ring-Down Spectroscopy

The most straightforward implementation of an intracavity element involves an off-the-shelf, commercially available BK7 Dove prism. Reflection losses at the 45° entrance and exit faces can be minimized with a high-quality antireflection coating (the best available antireflection coatings have a reflectivity $R \leq 0.25\%$). A liquid flow-cell can be clamped leak-tight onto the TIR face of the prism. In the experimental demonstrations performed to date, only 10% of the original ring-down time of the empty linear cavity was retained after insertion of this Dove prism (11, 18). This geometry has been employed to study the adsorption kinetics of crystal violet (a positively charged dye) to the negatively charged silica surface (11). Although this study was performed using

a pulsed multimode CRDS, sensitivity was slightly improved in a follow-up study that employed a broadband CW laser and a repetition rate of 6 kHz (12).

Because much of the optical loss is caused by intracavity reflections, the use of Brewster's angles for entrance and exit faces is expected to lead to considerable improvements (15). However, for this geometry similar baseline noise levels (10^{-4} A.U.) were obtained. Brewster's-angle geometry has been used to probe the molecular adsorption and the thermodynamic properties of (competitive) binding of neutral and charged dyes to the silica surface (15). A potential medical application of EW-CRDS is the rapid diagnosis of hemoglobinurea by measuring the adsorption of hemoglobin, which is present in the urine of hemoglobinurea patients, to the silica interface. Using this technique, one can detect concentrations of hemoglobin as small as 6 nM (13). An elegant way to probe the interfacial pH (which may be different from its bulk value) is through the covalent attachment of a pH-sensitive dye containing a triethoxysilane group to the silica surface. Titration of the surface influences the measured absorbance, allowing the interfacial pH to be probed (88).

As noted above, the antireflection coating on standard Dove prisms is only optimized for one polarization. Also, for Brewster's-angle prisms the reflection goes to zero for one polarization only. Consequently, these geometries cannot be used for polarization-dependent studies. For this purpose, a geometry with 90° entrance and exit faces can be utilized. Baseline noise levels on the order of 0.3×10^{-4} (17), 0.5×10^{-4} (89), and 3×10^{-4} (14) A.U. (all determined with pulsed multimode CRDS) can be achieved, and both polarizations can be used, enabling molecular orientation studies (14, 17, 89).

The molecular orientation of methylene blue at the air/silica interface can be measured after deposition of a methylene blue solution followed by solvent evaporation (89). For low coverage—up to one-fiftieth of a monolayer—the molecules lie almost flat on the surface, whereas they become more vertically oriented for higher surface coverages. For hemoglobin, investigators have studied both the adsorption from a static solution and the orientation of the adsorbed molecules (14). The orientation of the hemoglobin molecules changes during prolonged adsorption. Initially, an average tilt angle of 54.8° was measured; this angle increased to 57.9° during the course of the experiment (14). The initial value is close to the apparent orientation of 54.7° for randomly oriented molecules (the so-called magic angle) (89), which suggests that a random orientation is observed at the beginning of the adsorption process.

Silica surfaces can contain two types of silanol groups: 80% of the hydroxyl groups on hydroxylated surfaces are vicinal (SiOH), and 20% are geminal [$Si(OH)_2$]. The adsorption isotherm of crystal violet to silica can therefore be fitted to a two-site Langmuir equation (16); thus, two types of saturation densities and adsorption equilibrium constants are obtained. Such a two-site adsorption isotherm is not observed for small molecules that seem to interact with only one silanol group exclusively (15). For crystal violet, the average orientation of the molecules depends on the surface coverage and thus on the molecules' distribution between the two different sites (17).

In the aforementioned study (16), the positively charged crystal violet adsorption was employed for the indirect characterization of the negatively charged silanol groups, but crystal violet was also used in a study demonstrating that the amount of adsorption depends on the composition of the liquid on the prism surface (18). Most adsorption studies at the silica surface share the disadvantage that elaborate cleaning procedures must be performed after each measurement (12, 14, 17). However, in analytical chemistry, a better system would be one that can be applied during repeated measurements. It has been demonstrated that the addition of an organic modifier (in this case, methanol) to the liquid flow ensures a reversible chromatography-like adsorption process (18), thereby minimizing contamination or degradation. The same surface can be used over a prolonged time (days) without cleaning or realignment. In addition, superpolishing of the

TIR face did not result in a decrease of scatter losses, as these losses are primarily the result of intracavity surfaces. Unexpectedly, the amount of crystal violet adsorption was found to be lower on the superpolished prism. This may be because a larger surface area provides more binding sites for crystal violet. Another possibility is that on a rough surface, the liquid flow is turbulent, rather than laminar, which ensures more efficient exchange between crystal violet molecules in the solution and on the surface.

To date, EW-CRDS has been utilized mainly for studying adsorption kinetics and the molecular orientation of molecules at the silica surface. However, EW-CRDS is an extremely powerful technique and has many potential applications that have not yet been explored. One such application is the investigation of polymer/solvent interactions (90). When a polydimethylsiloxane film is placed on the TIR face of the prism, both the delamination and the additional scattering due to methanol diffusion in the film can be monitored (90).

Another promising application of EW-CRDS is the study of gold nanoparticle adsorption and aggregation kinetics at the silica/water interface (91). Gold nanoparticles can easily be synthesized using a citrate or borohydride reduction; the metastable colloidal solutions—which have an absorbance maximum in the visible range, where the surface plasmons of the particles are excited—then aggregate at the TIR surface. A refractive index sensor is obtained by immobilizing 0.32 of a colloid monolayer on the surface and subsequently monitoring the shift in surface plasmon resonance frequency at two different interrogation wavelengths. Refractive index changes of 0.3×10^{-5} can be detected (91, 92).

EW-CRDS can also be used in combination with other analytical techniques such as electrochemistry (16). This combination was accomplished by bringing an electrode close (25–250 μm) to the surface and electrogenerating strongly absorbing (at the measurement wavelength) $Fe(CN)_6^{3-}$ from weakly absorbing $Fe(CN)_6^{4-}$ ions. This setup allowed in situ monitoring of concentration changes accompanying electrochemical processes. After applying a step voltage, the time-dependent concentration changes of $Fe(CN)_6^{3-}$ were followed in real time. Increasing the electrode–prism surface distance results in a longer EW-CRDS time because the electrogenerated species must diffuse into the EW-CRDS-probing volume (16).

Ultimately, EW-CRDS may prove to be a valuable tool in label-free biosensing. As discussed above, aspecific EW-CRDS biosensing has already been demonstrated (13). This study exploits the fact that the positively charged hemoglobin molecules in a urine sample attach to the bare silica surface. However, any positively charged protein will aspecifically bind to the silica and the number of applications with silica surfaces as such is limited. A possible design for a EW-CRDS biosensor is schematically depicted in **Figure 7**. An important feature of this biosensor is that the TIR face of the prism should be modified. The modified prism should remain stable after prolonged exposure to a liquid flow, and the monolayer on the prism surface should not adversely affect the ring-down signal. Modifications such as the covalent attachment of a self-assembled monolayer (e.g., using trichloro- or triethoxyorganosilanes) or gel (e.g., a polycarboxylate hydrogel) that does not absorb at the measurement wavelength are useful for this purpose.

In an important exploratory study, Mazurenka et al. (19) demonstrated the feasibility of using modified prism surfaces in EW-CRDS. Although the aggregation of citrate-reduced gold colloidal solutions on the prism surface has been reported in the literature (91), the authors could not reproduce this aggregation, possibly because there were differences in the experimental procedures utilized. To facilitate the aggregation of the negatively charged colloids on the surface, the surface's polarity was reversed by prior aggregation of a positively charged poly-L-lysine layer. Although this type of surface modification relies on electrostatic interactions, no degradation of the surface monolayer was observed on repeated flushing with pure water (19). Addition of diluted colloidal solutions resulted in the deposition of a submonolayer of colloid particles on the surface, showing

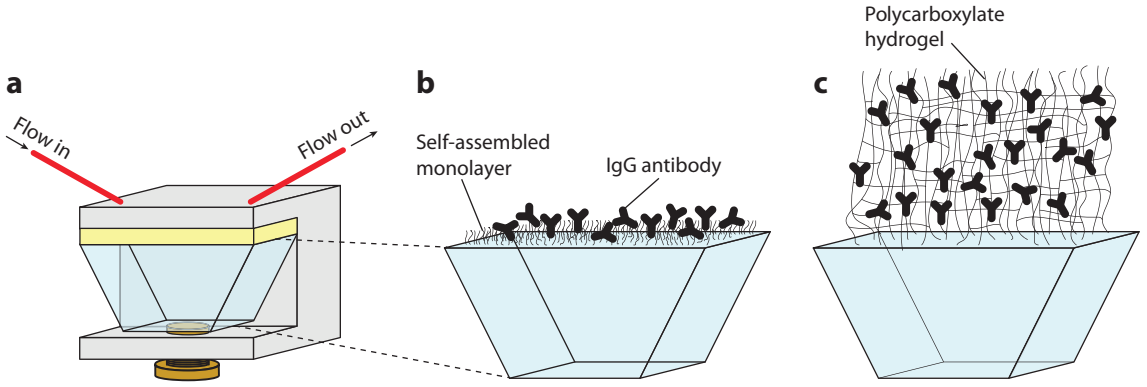

Figure 7

(*a*) A flow-cell is clamped leak-tight onto a surface-modified prism. Possible surface modifications are depicted in panels *b* and *c*. Bioactive molecules [in this case immunoglobin G (IgG) antibodies] are immobilized on the surface. Specific interactions with molecules, such as the binding of antigens to the immobilized antibodies, can be detected.

that even submonolayer densities can readily be detected. Multilayer deposition was achieved by repeating the poly-L-lysine deposition/colloid deposition steps on the same surface (19).

4.3. Evanescent-Wave Cavity Ring-Down Spectroscopy Using Fiber Cavities

Light traveling over a large distance in optical fibers attenuates as a result of processes such as absorption, scattering, and coupling into the cladding. Processes such as fiber bending or hydrogen diffusion in the fiber cause additional attenuation of light. With fiber CRDS or fiber-loop CRDS, one can measure losses other than direct absorption. In addition, when a part of the fiber cladding is removed, the exposed fiber core acts as an EW-sensing region.

Forces applied to the fiber cladding cause additional fiber losses, a phenomenon that has been utilized in the development of a fiber-loop ring-down pressure sensor (93). Alternatively, by introducing a biconical tapered region into the fiber loop, one can devise a fiber ring-down strain gauge (94). This device is similar to the pressure sensor: Bending the biconical taper causes an attenuation of the transmitted light, which allows the application of strain to be measured.

A fiber cavity is obtained when the two fiber ends (equipped with fiber-connector facets) are covered with high-reflectivity mirror coatings (95–97). Ring-down times thus obtained appear to depend on the degree of bending (95), which allows measurements of bending loss (97). Examples demonstrating the feasibility of EW sensing include (*a*) the measurement of the decrease in ring-down time during hydrogen fluoride etching (95) and (*b*) the measurement of hydrogen diffusion out of a fiber after loading the fiber in a hydrogen atmosphere (96). The H_2-loaded fiber showed a distinct absorption spectrum compared to the "clean" fiber (96).

Using specialized mirror coatings on fiber ends is not only expensive, it results in relatively high light losses: Reflections from the dielectric mirrors can be coupled in the cladding rather than the core. As an alternative approach, Gupta et al. (98) constructed a fiber cavity using two fiber-Bragg gratings. To test the performance of this fiber cavity, the authors manufactured an EW-sensing region and induced optical losses by varying the refractive index of the surrounding medium, demonstrating a sensitivity 100 times higher than that of a single-pass measurement (98).

A fiber-loop cavity with a biconical tapered region has been used for measuring an overtone absorption of 1-octyne, into which the biconical taper was dipped (99). Comparison with a

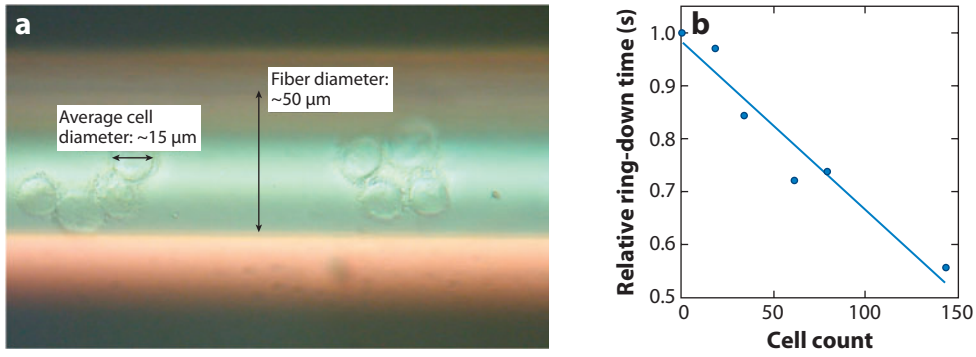

Figure 8

(*a*) Microscope image of cells adsorbed to the biconical taper. (*b*) Decrease in ring-down time as a function of the number of cells adsorbed to the taper. Reproduced with permission from Reference 100. Copyright 2005, American Institute of Physics.

low-resolution absorption spectrum recorded with a single-pass Fourier transform infrared spectrometer (utilizing a pathlength of 1 mm) showed qualitative agreement. In another study (100), detection of single cells adsorbed to the poly-L-lysine coated biconical taper was demonstrated. Cells that are adsorbed to the taper (**Figure 8*a***) gave rise to scattering of the evanescent field, thus decreasing the ring-down time (**Figure 8*b***); even the adsorption of a single cell could be detected (signal-to-noise ratio of 5).

5. FUTURE TRENDS AND PERSPECTIVES

CRDS, an exceptionally sensitive mode of absorption spectroscopy, is an increasingly valuable tool in liquid-phase analytical chemistry. It has already been shown that CRDS can significantly improve the sensitivity in LC absorbance detection in the visible range. Unfortunately, currently available mirrors are still insufficiently reflective to improve the performance in the ultraviolet range below 300 nm, where most analytes absorb. However, progress in mirror-coating technology is expected to bring about further improvements.

There are three main schemes for CRDS detection in LC: (*a*) a liquid-only cavity, (*b*) a flow-cuvette at 0° in a linear cavity, and (*c*) a Brewster's-angle flow-cell in a linear cavity. Because most LC studies make use of gradient flow systems in which the eluent composition is continuously changing, the detection scheme utilized should be insensitive to refractive index changes. Fiber-loop CRDS is especially useful where small detection volumes are involved, for example in capillary electrophoresis. Ultralow flow-cell volumes can be easily obtained using commercially available splice connectors.

The development of CW-CRDS promises to further improve sensitivity. Using this method, the repetition rate of the measurement can in principle be increased dramatically so as to strongly enhance the signal-to-noise ratio. However, due to the current speed of data transfer and processing, the repetition rate remains limited to approximately 1 kHz. When higher repetition rates are employed, multiple curves are averaged before data transfer; handling thus reduces the sensitivity. Currently, attainable baseline noise levels using CW-CRDS are only slightly better than those of conventional pulsed multimode CRDS schemes. The development of faster analog-to-digital conversion, fit algorithms, and data transfer promises to significantly improve the sensitivity of CW-CRDS.

A drawback of CRDS is that narrowbanded high-reflectivity dielectric mirrors must be used: The usable wavelength range is typically only 10% of the design wavelength. However, analytical absorbance detection sensitivity has already been improved through the use of a laser wavelength tuned 13 nm off the design wavelength of 470 nm, which suggests a certain freedom in the choice of the measurement wavelength.

Especially promising are current developments in IBB-CEAS, as this technique utilizes mirrors with a lower reflectivity but a broader wavelength range. Obtaining spectral information over a broader range of wavelengths is especially useful in condensed-media studies, where absorbance bands are usually much broader than in the gas phase. Surprisingly, the lowest (steady-state) LOD obtained for a convenient and affordable liquid-phase IBB-CEAS geometry (using a narrowband LED and a 99% mirror set) is only five times poorer than the LOD obtained using a more elaborate laser-based pulsed multimode CRDS as an LC detector at a single wavelength. Fiber-loop CRDS, which does not make use of mirrors at all, also has great potential. Unfortunately, the fibers are only transparent in the red and near-infrared, thus limiting fiber-loop CRDS measurements to those wavelengths.

Although the first exploratory experiments were performed more than a decade ago, the number of EW-CRDS studies in analytical chemistry remains limited. However, publications on the feasibility of, for instance, the combination of electrochemistry with EW-CRDS or remote in situ EW-CRDS sensing during thin-film growth demonstrate that EW-CRDS has the potential to become a useful and versatile tool. It is an especially appealing approach in that it combines the surface specificity of EW techniques with the excellent sensitivity of CRDS. To date, however, most studies concerning EW-CRDS used intracavity prisms, which, unfortunately, are prone to reflection and scatter losses, thus limiting the detection sensitivity. In the near future, the sensitivity will increase significantly when designs with inherently less scatter and reflection losses, such as a folded cavity or a fiber-loop cavity, are employed.

Although EW-CRDS is relatively new, EW absorption spectroscopy techniques such as waveguide spectroscopy and ATR spectroscopy are more mature. These techniques can also be combined with other spectroscopies, such as Raman and TIR fluorescence spectroscopy. Furthermore, many studies on chemically modified surfaces have been reported. Their basic principles are quite similar to those of EW-CRDS. Nonetheless, up-to-date EW-CRDS experiments are still limited to interaction studies of (bio)molecules with the bare silica surface. The application of existing knowledge concerning modifications of the TIR surface or the combination of various spectroscopies is currently underutilized. For instance, covalent attachment of monolayers to the TIR surface may provide insight into interactions with surfaces other than silica. Ultimately, the immobilization of biomolecules on the surface may facilitate biospecific label-free EW-CRDS detection.

DISCLOSURE STATEMENT

The authors are not aware of any affiliations, memberships, funding, or financial holdings that might be perceived as affecting the objectivity of this review.

ACKNOWLEDGMENTS

Financial support from the Netherlands Foundation for Fundamental Research of Matter (FOM) is gratefully acknowledged.

LITERATURE CITED

1. Hallock AJ, Berman ESF, Zare RN. 2002. Direct monitoring of absorption in solution by cavity ring-down spectroscopy. *Anal. Chem.* 74:1741–43
2. Snyder KL, Zare RN. 2003. Cavity ring-down spectroscopy as a detector for liquid chromatography. *Anal. Chem.* 75:3086–91
3. Bechtel KL, Zare RN, Kachanov AA, Sanders SS, Paldus BA. 2005. Moving beyond traditional UV-visible absorption detection: cavity ring-down spectroscopy for HPLC. *Anal. Chem.* 77:1177–82
4. Bahnev B, van der Sneppen L, Wiskerke AE, Ariese F, Gooijer C, Ubachs W. 2005. Miniaturized cavity ring-down detection in a liquid flow-cell. *Anal. Chem.* 77:1188–91
5. van der Sneppen L, Wiskerke A, Ariese F, Gooijer C, Ubachs W. 2006. Improving the sensitivity of HPLC absorption detection by cavity ring down spectroscopy in a liquid-only cavity. *Anal. Chim. Acta* 558:2–6
6. van der Sneppen L, Wiskerke A, Ariese F, Gooijer C, Ubachs W. 2006. Cavity ring-down spectroscopy for detection in liquid chromatography: extension to tunable sources and UV wavelengths. *Appl. Spectrosc.* 60:935–38
7. van der Sneppen L, Ariese F, Gooijer C, Ubachs W. 2007. Cavity ring-down spectroscopy for detection in liquid chromatography at UV wavelengths using standard cuvettes in a normal incidence geometry. *J. Chromatogr. A* 1148:184–88
8. Pipino ACR, Hudgens JW, Huie RE. 1997. Evanescent wave cavity ring-down spectroscopy with a total-internal-reflection minicavity. *Rev. Sci. Instrum.* 68:2978–89
9. Pipino ACR. 1999. Ultrasensitive surface spectroscopy with a miniature optical resonator. *Phys. Rev. Lett.* 83:3093–96
10. Pipino ACR. 2000. Monolithic folded resonator for evanescent wave cavity ringdown spectroscopy. *Appl. Opt.* 39:1449–53
11. Shaw AM, Hannon TE, Li F, Zare RN. 2003. Adsorption of crystal violet to the silica-water interface monitored by evanescent wave cavity ring-down spectroscopy. *J. Phys. Chem. B* 107:7070–75
12. Fisk JD, Batten R, Jones G, O'Reilly JP, Shaw AM. 2005. pH dependence of the crystal violet adsorption isotherm at the silica-water interface. *J. Phys. Chem. B* 109:14475–80
13. Martin WB, Mirov S, Martyshkin D, Venugopalan R. 2005. Hemoglobin adsorption isotherm at the silica-water interface with evanescent wave cavity ring-down spectroscopy. *J. Biomed. Opt.* 10:024025
14. Everest MA, Black VM, Haehlen AS, Haveman GA, Kliewer CJ, Neill HA. 2006. Hemoglobin adsorption to silica monitored with polarization-dependent evanescent-wave cavity ring-down spectroscopy. *J. Phys. Chem. B* 110:19461–68
15. Fan H-F, Hung C-Y, Lin K-C. 2006. Molecular adsorption at silica/CH_3 CN interface probed by using evanescent wave cavity ring-down absorption spectroscopy: determination of thermodynamic properties. *Anal. Chem.* 78:3583–90
16. Mazurenka M, Wilkins L, Macpherson JV, Unwin PR, Mackenzie SR. 2006. Evanescent wave cavity ring-down spectroscopy in a thin-layer electrochemical cell. *Anal. Chem.* 78:6833–39
17. Fan H-F, Li F, Zare RN, Lin K-C. 2007. Characterization of two types of silanol groups on fused-silica surfaces using evanescent-wave cavity ring-down spectroscopy. *Anal. Chem.* 79:3654–61
18. van der Sneppen L, Buijs J, Gooijer C, Ubachs W, Ariese F. 2008. Evanescent-wave cavity ring-down spectroscopy for enhanced detection of surface binding under flow injection analysis conditions. *Appl. Spectrosc.* 62:649–54
19. Mazurenka M, Hamilton SM, Unwin PR, Mackenzie SR. 2008. In-situ measurement of colloidal gold adsorption on functionalized silica surfaces. *J. Phys. Chem. C* 112:6462–68
20. Herriot D, Kogelnik H, Kompfner R. 1964. Off-axis paths in spherical mirror interferometers. *Appl. Opt.* 3:523–26
21. White J. 1942. Long optical paths of large aperture. *J. Opt. Soc. Am.* 32:285–88
22. Poole C, Poole SK. 1991. *Chromatography Today*. Amsterdam: Elsevier
23. Gooijer C, Hoornweg GP, de Beer T, Bader A, van Iperen DJ, Brinkman UAT. 1998. Detector cell based on plastic liquid-core waveguides suitable for aqueous solutions: one-to-two decades improved detection limits in conventional-size column liquid chromatography with absorption detection. *J. Chromatogr. A* 824:1–5

24. Dallas T, Dasgupta PK. 2004. Light at the end of the tunnel: recent analytical applications of liquid-core waveguides. *Trends Anal. Chem.* 23:385–92
25. de Beer T, Velthorst NH, Brinkman UAT, Gooijer C. 2002. Laser-based nonfluorescence detection techniques for liquid separation systems. *J. Chromatogr. A* 971:1–35
26. Navas MJ, Jimenez AM. 2003. Thermal lens spectrometry as analytical tool. *Crit. Rev. Anal. Chem.* 33:77–88
27. Li F, Kachanov AA, Zare RN. 2007. Detection of separated analytes in subnanoliter volumes using coaxial thermal lensing. *Anal. Chem.* 79:5264–71
28. Wu J, Odake T, Kitamori T, Sawada T. 1991. Ultrasensitive detection for capillary zone electrophoresis using laser-induced capillary vibration. *Anal. Chem.* 63:2216–18
29. Rey JM, Sigrist MW. 2007. Differential mode excitation photoacoustic spectroscopy: A new photoacoustic detection scheme. *Rev. Sci. Instrum.* 78:063104
30. Farrow RL, Rakestraw DJ. 1992. Detection of trace-molecular species using degenerate 4-wave mixing. *Science* 257:1894–900
31. Hoornweg GP, de Beer T, Velthorst NH, Gooijer C. 1997. Forward degenerate four-wave mixing as a detection method in liquid separation systems: Improving detection limits by means of a Fabry-Perot interferometer. *Appl. Spectrosc.* 51:1008–11
32. Herbelin JM, McKay JA, Kwok MA, Uenten RH, Urevig DS, et al. 1980. Sensitive measurement of photon lifetime and true reflectances in an optical cavity by a phase-shift method. *Appl. Opt.* 19:144–47
33. Anderson DZ, Frisch JC, Masser CS. 1984. Mirror reflectometer based on optical cavity decay time. *Appl. Opt.* 23:1238–45
34. O'Keefe A, Deacon DAG. 1988. Cavity ring-down optical spectrometer for absorption measurements using pulsed laser sources. *Rev. Sci. Instrum.* 59:2544–51
35. Paldus B, Kachanov A. 2005. An historical overview of cavity-enhanced methods. *Can. J. Phys.* 83:975–99
36. Atkinson D. 2003. Solving chemical problems of environmental importance using cavity ring-down spectroscopy. *Analyst* 128:117–25
37. Brown S. 2003. Absorption spectroscopy in high-finesse cavities for atmospheric studies. *Chem. Rev.* 103:5219–38
38. Berden G, Peeters R, Meijer G. 2000. Cavity ring-down spectroscopy: experimental schemes and applications. *Int. Rev. Phys. Chem.* 19:565–607
39. Busch K, Busch M. 1999. *Cavity Ring-Down Spectroscopy: An Ultratrace Absorption Measurement Technique*. Oxford, UK: Oxford Univ. Press
40. Wheeler MD, Newman SM, Orr-Ewing AJ, Ashfold MNR. 1998. Cavity ring-down spectroscopy. *Faraday Trans.* 94:337–51
41. Scherer J, Paul J, O'Keefe A, Saykally R. 1997. Cavity ringdown laser absorption spectroscopy: history, development, and application to pulsed molecular beams. *Chem. Rev.* 97:25–51
42. Ball SM, Jones RL. 2003. Broad-band cavity ring-down spectroscopy. *Chem. Rev.* 103:5239–63
43. Crosson ER, Ricci KN, Richman BA, Chilese FC, Owano TG, et al. 2002. Stable isotope ratios using cavity ring-down spectroscopy: determination of $^{13}C/^{12}C$ for carbon dioxide in human breath. *Anal. Chem.* 74:2003–7
44. von Basum G, Dahnke H, Halmer D, Hering P, Mürtz M. 2003. Online recording of ethane traces in human breath via infrared laser spectroscopy. *J. Appl. Phys.* 95:2583–90
45. Dahnke H, Kleine D, Hering P, Mürtz M. 2001. Real-time monitoring of ethane in human breath using mid-infrared cavity leak-out spectroscopy. *Appl. Phys. B* 72:971–75
46. Vallance C. 2005. Innovations in cavity ringdown spectroscopy. *New J. Chem.* 29:867–74
47. Kraning CM, Benz TL, Bloome KS, Campanello GC, Fahrenbach VS, et al. 2007. Determination of surface coverage and orientation of reduced cytochrome c on a silica surface with polarized ATR spectroscopy. *J. Phys. Chem. C* 111:13062–67
48. Walker DS, Hellinga HW, Saavedra SS, Reichert WM. 1993. Integrated optical waveguide attenuated total reflection spectrometry and resonance Raman spectroscopy of adsorbed cytochrome c. *J. Phys. Chem.* 97:10217–22
49. Edminston PL, Lee JE, Cheng S-S, Saavedra SS. 1997. Molecular orientation distributions in protein films. 1. Cytochrome c adsorbed to substrates of variable surface chemistry. *J. Am. Chem. Soc.* 119:560–70

50. Hook F, Voros J, Rodahl M, Kurrat R, Boni P, et al. 2002. A comparative study of protein adsorption on titanium oxide surfaces using in situ ellipsometry, optical waveguide lightmode spectroscopy, and quartz crystal microbalance/dissipation. *Colloids Surf. B* 24:155–70
51. Kogelnik H, Li T. 1966. Laser beams and resonators. *Appl. Opt.* 5:1550–67
52. Demtröder W. 2003. *Laser Spectroscopy*. Berlin-Heidelberg: Springer
53. Naus H, van Stokkum IHM, Hogervorst W, Ubachs W. 2001. Quantitative analysis of decay transients applied to a multimode pulsed cavity ringdown experiment. *Appl. Opt.* 40:4416–26
54. Meijer G, Boogaarts M, Jongma R, Parker D. 1994. Coherent cavity ring down spectroscopy. *Chem. Phys. Lett.* 217:112–16
55. van Zee RD, Hodges JT, Looney JP. 1999. Pulsed, single-mode cavity ringdown spectroscopy. *Appl. Opt.* 38:3951–60
56. Romanini D, Kachanov AA, Sadeghi N, Stoeckel F. 1997. CW-cavity ring down spectroscopy. *Chem. Phys. Lett.* 264:316–22
57. Romanini D, Kachanov AA, Stoeckel F. 1997. Diode laser cavity ring down spectroscopy. *Chem. Phys. Lett.* 270:538–45
58. Romanini D, Kachanov AA, Stoeckel F. 1997. Cavity ring down spectroscopy: broad band absolute absorption measurements. *Chem. Phys. Lett.* 270:546–50
59. O'Keefe A, Scherer JJ, Paul JB. 1999. CW integrated cavity output spectroscopy. *Chem. Phys. Lett.* 307:343–49
60. Gherman T, Romanini D. 2002. Mode-locked cavity-enhanced absorption spectroscopy. *Opt. Express* 10:1033–42
61. Gherman T, Romanini D, Sagnes I, Garnache A, Zhang Z. 2004. Cavity-enhanced absorption spectroscopy with a mode-locked diode-pumped vertical external-cavity surface-emitting laser. *Chem. Phys. Lett.* 390:290–95
62. Fiedler S, Hoheisel G, Ruth A, Hese A. 2003. Incoherent broad-band cavity-enhanced absorption spectroscopy of azulene in a supersonic jet. *Chem. Phys. Lett.* 382:447–53
63. Ball SM, Langridge JM, Jones RL. 2004. Broadband cavity enhanced absorption spectroscopy using light emitting diodes. *Chem. Phys. Lett.* 398:68–74
64. Islam M, Seetohul L, Ali Z. 2007. Liquid-phase broadband cavity enhanced absorption spectroscopy measurements in a 2 mm cuvette. *Appl. Spectrosc.* 61:649–58
65. Fiedler S, Hese A, Ruth A. 2005. Incoherent broad-band cavity-enhanced absorption spectroscopy of liquids. *Rev. Sci. Instrum.* 76:023107
66. Engeln R, von Helden G, van Roij A, Meijer G. 1999. Cavity ring down spectroscopy on solid C_{60}. *J. Chem. Phys.* 110:2732–33
67. Egashira K, Terasaki A, Kondow T. 2007. Infrared spectra of organic monolayer films in a standing wave measured by photon-trap spectroscopy. *J. Chem. Phys.* 126:221102
68. Kleine D, Lauterbach J, Kleinermanns K, Hering P. 2001. Cavity ring-down spectroscopy of molecularly thin iodine layers. *Appl. Phys. B* 72:249–52
69. Xu S, Sha G, Xie J. 2002. Cavity ring-down spectroscopy in the liquid phase. *Rev. Sci. Instrum.* 73:255–58
70. Fiedler S, Hese A, Ruth A. 2003. Incoherent broad-band cavity-enhanced absorption spectroscopy. *Chem. Phys. Lett.* 371:284–94
71. Hallock AJ, Berman ESF, Zare RN. 2003. Ultratrace kinetic measurements of the reduction of methylene blue. *J. Am. Chem. Soc.* 125:1158–59
72. Hallock AJ, Berman ESF, Zare RN. 2003. Use of broadband, continuous-wave diode lasers in cavity ring-down spectroscopy for liquid samples. *Specif. Tech.* 57:571–73
73. Alexander AJ. 2004. Reaction kinetics of nitrate radicals with terpenes in solution studied by cavity ring-down spectroscopy. *Chem. Phys. Lett.* 393:138–42
74. Alexander A. 2006. Flowing liquid-sheet jet for cavity ring-down absorption measurements. *Anal. Chem.* 78:5597–600
75. Fiedler SE, Hese A, Heitmann U. 2007. Influence of the cavity parameters on the output intensity in incoherent broadband cavity-enhanced absorption spectroscopy. *Rev. Sci. Instrum.* 78:073104
76. McGarvey T, Conjusteau A, Mabuchi H. 2006. Finesse and sensitivity gain in cavity-enhanced absorption spectroscopy of biomolecules in solution. *Opt. Express* 14:10441–51

77. Brown R, Kozin I, Tong Z, Oleschuk R, Loock H-P. 2002. Fiber-loop ring-down spectroscopy. *J. Chem. Phys.* 117:10444–47
78. Loock H-P. 2006. Ring-down absorption spectroscopy for analytical microdevices. *Trends Anal. Chem.* 25:655–64
79. Tong Z, Wright A, McCormick T, Li R, Oleschuk R, Loock H-P. 2004. Phase-shift fiber-loop ring-down spectroscopy. *Anal. Chem.* 76:6594–99
80. Li R, Loock H-P, Oleschuk RD. 2006. Capillary electrophoresis absorption detection using fiber-loop ring-down spectroscopy. *Anal. Chem.* 78:5685–92
81. Andachi M, Nakayama T, Kawasaki M, Kurokawa S, Loock H-P. 2007. Fiber-optic ring-down spectroscopy using a tunable picosecond gain-switched diode laser. *Appl. Phys. B* 88:131–35
82. Schiller S, Yu II, Fejer MM, Byer RL. 1992. Fused-silica monolithic total-internal-reflection resonator. *Opt. Lett.* 17:378–80
83. Pipino A, Michalski M. 2007. Climbing the vibrational ladder to probe the OH stretch of HNO_3 on silica. *J. Phys. Chem. C* 111:9442–47
84. Aarts IMP, Pipino ACR, Hoefnagels JPM, Kessels WMM, van de Sanden MCM. 2005. Quasi-ice monolayer on atomically smooth amorphous SiO_2 at room temperature observed with a high-finesse optical resonator. *Phys. Rev. Lett.* 95:166104
85. Pipino ACR, Hoefnagels JPM, Watanabe N. 2004. Absolute surface coverage measurement using a vibrational overtone. *J. Chem. Phys.* 120:2879–88
86. Bolis V, Cavenago A, Fubini B. 1997. Surface heterogeneity on hydrophilic and hydrophobic silicas: water and alcohols as probes for H-bonding and dispersion forces. *Langmuir* 13:895
87. Aarts I, Pipino A, van de Sanden M, Kessels W. 2007. Absolute in-situ measurements of surface dangling bonds during a Si:H growth. *Appl. Phys. Lett.* 90:161918
88. O'Reilly JP, Butts CP, l'Anson IA, Shaw AM. 2005. Interfacial ph at an isolated silica-water surface. *J. Am. Chem. Soc. Commun.* 127:1632–33
89. Li F, Zare RN. 2005. Molecular orientation study of methylene blue at an air/fused-silica interface using evanescent-wave cavity ring-down spectroscopy. *J. Phys. Chem. B* 109:3330–33
90. Hannon TE, Chah S, Zare RN. 2005. Evanescent-wave cavity ring-down investigation of polymer/solvent interactions. *J. Phys. Chem. B* 109:7435–42
91. Fisk JD, Rooth M, Shaw AM. 2007. Gold nanoparticle adsorption and aggregation kinetics at the silica-water interface. *J. Phys. Chem. C* 111:2588–94
92. O'Reilly JP, Fisk JD, Rooth M, Perkins E, Shaw AM. 2007. Non-linear plasmon response to protein binding at a nanostructured gold particle plasmon resonance surface. *Phys. Chem. Chem. Phys.* 9:344–45
93. Wang C, Scherrer ST. 2004. Fiber ringdown pressure sensors. *Opt. Lett.* 29:352–54
94. Tarsa PB, Brzozowski DM, Rabinowitz P, Lehmann KK. 2004. Cavity ringdown strain gauge. *Opt. Lett.* 29:1339–41
95. von Lerber T, Sigrist MW. 2002. Cavity ring-down principle for fiber-optic resonators: experimental realization of bending loss and evanescent-field sensing. *Appl. Opt.* 41:3567–75
96. Vogler DE, Müller MG, Sigrist MW. 2003. Fiber-optic cavity sensing of hydrogen diffusion. *Appl. Opt.* 42:5413–17
97. Vogler DE, Lorencak A, Rey JM, Sigrist MW. 2005. Bending loss measurement using a fiber cavity ringdown scheme. *Opt. Lasers Eng.* 43:527–35
98. Gupta M, Jiao H, O'Keefe A. 2002. Cavity-enhanced spectroscopy in optical fibers. *Opt. Lett.* 27:1878–80
99. Tarsa PB, Rabinowitz P, Lehmann KK. 2004. Evanescent field absorption in a passive optical fiber resonator using continuous-wave cavity ring-down spectroscopy. *Chem. Phys. Lett.* 383:297–303
100. Tarsa PB, Wist AD, Rabinowitz P, Lehmann KK. 2004. Single-cell detection by cavity ring-down spectroscopy. *Appl. Phys. Lett.* 85:452325

Annual Review of
Analytical Chemistry

Volume 2, 2009

Contents

A Conversation with John B. Fenn
John B. Fenn and M. Samy El-Shall 1

Liquid-Phase and Evanescent-Wave Cavity Ring-Down Spectroscopy in Analytical Chemistry
L. van der Sneppen, F. Ariese, C. Gooijer, and W. Ubachs 13

Scanning Tunneling Spectroscopy
Harold J. W. Zandvliet and Arie van Houselt 37

Nanoparticle PEBBLE Sensors in Live Cells and In Vivo
Yong-Eun Koo Lee, Ron Smith, and Raoul Kopelman 57

Micro- and Nanocantilever Devices and Systems for Biomolecule Detection
Kyo Seon Hwang, Sang-Myung Lee, Sang Kyung Kim, Jeong Hoon Lee, and Tae Song Kim 77

Capillary Separation: Micellar Electrokinetic Chromatography
Shigeru Terabe 99

Analytical Chemistry with Silica Sol-Gels: Traditional Routes to New Materials for Chemical Analysis
Alain Walcarius and Maryanne M. Collinson 121

Ionic Liquids in Analytical Chemistry
Renee J. Soukup-Hein, Molly M. Warnke, and Daniel W. Armstrong 145

Ultrahigh-Mass Mass Spectrometry of Single Biomolecules and Bioparticles
Huan-Cheng Chang 169

Miniature Mass Spectrometers
Zheng Ouyang and R. Graham Cooks 187

Analysis of Genes, Transcripts, and Proteins via DNA Ligation
Tim Conze, Alysha Shetye, Yuki Tanaka, Jijuan Gu, Chatarina Larsson, Jenny Göransson, Gholamreza Tavoosidana, Ola Söderberg, Mats Nilsson, and Ulf Landegren 215

Applications of Aptamers as Sensors
Eun Jeong Cho, Joo-Woon Lee, and Andrew D. Ellington 241

Mass Spectrometry–Based Biomarker Discovery: Toward a Global Proteome Index of Individuality
Adam M. Hawkridge and David C. Muddiman 265

Nanoscale Control and Manipulation of Molecular Transport in Chemical Analysis
Paul W. Bohn 279

Forensic Chemistry
Suzanne Bell 297

Role of Analytical Chemistry in Defense Strategies Against Chemical and Biological Attack
Jiri Janata 321

Chromatography in Industry
Peter Schoenmakers 333

Electrogenerated Chemiluminescence
Robert J. Forster, Paolo Bertoncello, and Tia E. Keyes 359

Applications of Polymer Brushes in Protein Analysis and Purification
Parul Jain, Gregory L. Baker, and Merlin L. Bruening 387

Analytical Chemistry of Nitric Oxide
Evan M. Hetrick and Mark H. Schoenfisch 409

Characterization of Nanomaterials by Physical Methods
C.N.R. Rao and Kanishka Biswas 435

Detecting Chemical Hazards with Temperature-Programmed Microsensors: Overcoming Complex Analytical Problems with Multidimensional Databases
Douglas C. Meier, Baranidharan Raman, and Steve Semancik 463

The Analytical Chemistry of Drug Monitoring in Athletes
Larry D. Bowers 485

Errata

An online log of corrections to *Annual Review of Analytical Chemistry* articles may be found at http://anchem.annualreviews.org/errata.shtml